# *Rhodospirillum rubrum* CO-Dehydrogenase. Part 1. Spectroscopic Studies of CODH Variant C531A Indicate the Presence of a Binuclear [FeNi] Cluster

**Christopher R. Staples,[‡] Jongyun Heo,[‡] Nathan J. Spangler,[‡] Robert L. Kerby,[§] Gary P. Roberts,[§] and Paul W. Ludden\*,[‡]**

*Contribution from the Departments of Biochemistry and Bacteriology, College of Agricultural and Life Sciences, University of Wisconsin-Madison, Madison, Wisconsin 53706*

*Received February 8, 1999. Revised Manuscript Received July 30, 1999*

**Abstract:** A variant of the carbon monoxide dehydrogenase (CODH) from *Rhodospirillum rubrum* was constructed by site-directed mutagenesis of the *cooS* gene to yield a CODH with ala in place of cys-531. This variant form of CODH (C531A) has a metal content identical to that of wild-type CODH but has an extremely slow turnover rate. Cys-531 is not essential for construction of the $[Fe_4S_4]$ clusters or for incorporation of nickel. The $K_m$ for methyl viologen is identical to that of wild-type CODH, but the $K_m$ for CO is approximately 30% that of wild-type CODH. The data suggest that in C531A CODH a rate-limiting step has been introduced at the point of electron transfer from the Ni site to an associated $[Fe_4S_4]_C$ cluster. Examination of indigo carmine-poised, CO-pretreated C531A CODH revealed the presence of a paramagnetic species ($g = 2.33$, 2.10, 2.03; $g_{ave} = 2.16$), which was also observed in dithionite-treated samples. This species was shown to represent as much as $0.90 \pm 0.10$ spins/molecule, yet production of the species from fully oxidized C531A CODH did not involve a concurrent decrease in the molar extinction coefficient at 420 nm, indicating that the $[Fe_4S_4]$ clusters remained in the 2+ oxidation state. $^{61}Ni$-substituted CO-pretreated C531A CODH, when poised with indigo carmine, showed no broadening of the resonances, indicating that no detectable spin density resides upon Ni. Comparisons of the EPR spectrum of the $g_{ave} = 2.16$ species to Ni-C(CO) and Ni-C of *Alcaligenes eutrophus* [NiFe] hydrogenase are presented. On the basis of these comparisons and on the lack of $^{61}Ni$ broadening, the $g_{ave} = 2.16$ resonance is interpreted as arising from a $[(CO_L)Fe^{3+}-Ni^{2+}-H^-]^{4+}$ ($S = 1/2$) system, where $CO_L$ is an activating nonsubstrate CO ligand. On the basis of the absence of spectroscopic features present in wild-type CODH, and representing coupled forms of the putative [FeNi] cluster with a $[Fe_4S_4]$, cys-531 is proposed to be directly involved in the coupling of the putative [FeNi] site with the associated $[Fe_4S_4]$ cluster.

## Introduction

The CO-induced carbon monoxide dehydrogenase (CODH) of *Rhodospirillum rubrum* is the product of the *cooS* gene and is isolated as a 65 kDa monomer containing one Ni atom, 8−9 Fe atoms, and 8−9 atoms of acid-labile sulfur.[1,2] CODH is the key enzyme in the oxidation of CO to $CO_2$ as shown in eq 1,

$$CO + H_2O \rightleftarrows CO_2 + 2H^+ + 2e^- \qquad (1)$$

and it operates in conjunction with a CO-induced hydrogenase to allow *R. rubrum* to grow anaerobically in the dark with CO as the energy source.[1,3,4]

A diverse group of bacteria and archaea produce Ni-containing, CO-oxidizing enzymes, and all of these except the

CODH from *R. rubrum* play a central role in synthesis or catabolism of acetyl-coenzymeA. Thus, these other enzymes are referred to as acetylCoA synthases (ACS).[5] The ACSs are dimeric enzymes, one subunit of which is homologous to *R. rubrum* CODH.[6,7] The most studied ACS is that from the acetogen *Clostridium thermoaceticum*.[8−10] The $\beta$ subunit of the *C. thermoaceticum* ACS contains CODH activity and has EPR and Mössbauer spectra similar to those of *R. rubrum* CODH. The gene encoding the $\beta$ subunit in *C. thermoaceticum* (*cdhA*) and the *cooS* gene in *R. rubrum* share significant sequence similarity.[11] The $\alpha$ subunit of ACS enzymes contains the site of acetylCoA synthesis.

(1) Bonam, D.; Murrell, S. A.; Ludden, P. W. *J. Bacteriol.* **1984**, *159*, 693−699.
(2) Bonam, D.; Ludden, P. W. *J. Biol. Chem.* **1987**, *262*, 2980−2987.
(3) Bonam, D.; Lehman, L.; Roberts, G. P.; Ludden, P. W. *J. Bacteriol.* **1989**, *171*, 3102−3107.
(4) Kerby, R. L.; Ludden, P. W.; Roberts, G. P. *J. Bacteriol.* **1995**, *177*, 2241−2244.

(5) Wood, H. G.; Ragsdale, S. W.; Pezacka, E. *FEMS Microbiol. Rev.* **1986**, *39*, 345−362.
(6) Morton, T. A.; Runquist, J. A.; Ragsdale, S. W.; Chanmugasundaram, T.; Wood, H. G.; Ljungdahl, L. G. *J. Biol. Chem.* **1991**, *266*, 23824−23828.
(7) Ragsdale, S. W.; Clark, J. E.; Ljungdahl, L. G.; Lundie, L. L.; Drake, H. L. *J. Biol. Chem.* **1983**, *258*, 2364−2369.
(8) Gorst, C. M.; Ragsdale, S. W. *J. Biol. Chem.* **1991**, *266*, 20687−20693.
(9) Lindahl, P. A.; Münck, E.; Ragsdale, S. W. *J. Biol. Chem.* **1990**, *265*, 3873−3879.
(10) Lindahl, P. A.; Ragsdale, S. W.; E., M. *J. Biol. Chem.* **1990**, *265*, 3880−3888.
(11) Seravalli, J.; Kumar, M.; Lu, W.-P.; Ragsdale, S. W. *Biochemistry* **1995**, *34*, 7879−7888.

The metal clusters of *R. rubrum* CODH[12] and the CO-oxidizing subunit of ACS[13] have been characterized respectively as an $[Fe_4S_4]$ cluster termed the B cluster and as a Ni-X-$[Fe_4S_4]$ cluster referred to as the C cluster or C site, where "X" is an putative bridging ligand. Henceforth in this manuscript the $[Fe_4S_4]$ cluster at the C site will be designated $[Fe_4S_4]_C$. The B cluster serves as the conduit for electrons to pass to external electron acceptors and exhibits UV−vis, EPR, and Mössbauer spectra that are readily interpreted as arising from a fairly standard, cysteinyl-liganded $[Fe_4S_4]$ cluster (hereafter referred to as $[Fe_4S_4]_B$).[10,12] The B cluster has an accessible $[Fe_4S_4]^{2+/1+}$ redox couple with $E_m = -435$ mV versus the standard hydrogen electrode (SHE).

The C cluster is the site of CO oxidation and has been characterized as an unusually liganded $[Fe_4S_4]$ cluster bridged to the Ni atom by an unidentified ligand ("X"). ENDOR[14] and Mössbauer spectra[10] are consistent with the interpretation of a pentacoordinate Fe atom at one corner of $[Fe_4S_4]_C$ analogous to the $[Fe_4S_4]$ cluster of aconitase.[15] EXAFS studies have precluded the possibility of the Ni atom being located at one corner of the cubane (i.e., $[NiFe_3S_4]$).[16,17]

Several EPR signals exhibited by CODH have been attributed to the C cluster. These include $C_{red1}$ (apparent $g_{z,y,x} = 2.03$, 1.88, 1.71; $g_{ave} = 1.87$), which has been interpreted as arising from a $Ni^{2+}/[Fe_4S_4]_C^{1+}$ state of the cluster; $C_{red2}$ (apparent $g_x = 1.75$), which is also interpreted as $Ni^{2+}/[Fe_4S_4]_C^{1+}$; and "$C = {}^3/_2$", which is a more complex signal.[12,18,19] Neither the $C_{red1}$ nor $C_{red2}$ signals integrate to a unit spin, which has suggested that the signals arose from incomplete coupling or that they represented a percentage of the population of the C cluster. When CODH is treated with excess thionin ($E_m = +64$ mV), the C cluster is oxidized to a form called "$C_{ox}$", which has been interpreted as arising from a $Ni^{2+}/[Fe_4S_4]_C^{2+}$ state and is EPR-silent. Interconversion of $C_{ox}$ and $C_{red1}$ occurs with a midpoint potential of $-110$ mV versus SHE. The Ni atom of the C cluster does not contribute to the UV−vis spectrum of *R. rubrum* CODH, and to date, EPR spectra of CODH have been interpreted as indicating that Ni remains in the $Ni^{2+}$ state throughout the catalytic cycle. Data presented in this and the companion manuscript will challenge these interpretations.

The *R. rubrum* CODH can be obtained in an inactive, Ni-deficient form that contains $[Fe_4S_4]_B$ and $[Fe_4S_4]_C$.[20] Treatment of reduced ($[Fe_4S_4]_B^{1+}$, $[Fe_4S_4]_C^{1+}$) Ni-deficient-CODH with $Ni^{2+}$ results in full activation of the enzyme and restoration of the spectroscopic properties of the holo-form. Cobalt ($Co^{2+}$), $Zn^{2+}$, and $Fe^{2+}$ ions can be inserted in place of $Ni^{2+}$; only the cobalt form of the enzyme exhibits CO oxidation activity and that activity is very poor. Ni-deficient-CODH does not exhibit detectable $C_{red1}$ or $C_{red2}$ states, and the midpoint potential of the $[Fe_4S_4]_C^{2+/1+}$ couple in the absence of Ni is about $-430$

mV versus SHE. Thus, the presence of $Ni^{2+}$ results in a significant increase in the midpoint potential of $[Fe_4S_4]_C$.[18]

Sequences of genes for *R. rubrum* CODH (*cooS*) and for the CO-oxidizing subunits of ACS enzymes from at least a dozen sources are now available. The genes show significant sequence conservation and a number of absolutely conserved cys and his residues that might serve as metal ligands. The properties of a CODH variant in which cys-531 has been replaced by ala are reported here.

Spectroscopic analyses of CODH and [NiFe] hydrogenases have proceeded in parallel for many years, but little interchange of ideas has occurred. The recent elucidation of the structure of the *Desulfovibrio gigas* [NiFe] hydrogenase[21] has led us to consider possible similarities between the two systems. Data in this and the companion manuscript suggest that *R. rubrum* CODH contains a [FeNi] binuclear cluster in addition to $[Fe_4S_4]_C$ and $[Fe_4S_4]_B$ and that it is primarily the Fe atom of the [FeNi] cluster that is redox active during catalysis. Spin couplings between pairs of the three clusters give rise to the enigmatic $C_{red1}$ and $C_{red2}$ signals. These results allow the proposal of a mechanism that accounts for a two-electron transfer from substrate (CO) to the enzyme without invoking an EPR-silent center (sometimes referred to as "X" or "S") or intermediate redox state (termed "$C_{int}$") in the enzyme.

## Experimental Procedures

**Mutant Construction.** The mutant producing C531A CODH was constructed using the restriction-site-elimination method[22] with some modifications.[23] Media and antibiotic usage have been described.[24] The pUC19-derived template plasmid (pCO11, in *E. coli* strain UQ1155) bears a 2.2-kb *Sal*I fragment that encompasses all of *cooS*, the gene encoding *R. rubrum* CODH. This template was mutagenized in vitro using a selection primer, which converted an *Afl*III site to a *Bgl*II site in the vector, and a mutagenic primer, which converted the cys-531 codon (TGC) to an ala (GCC) in *cooS*. The mutated *cooS*, verified by sequence analysis, was excised as a 1.2-kb *Nco*I to *Hin*dIII fragment and then cloned into similarly digested pCO12R (*E. coli* strain UQ1161), which bears *coo* DNA extending 2.0 kb upstream of the *Nco*I site and 1.6 kb downstream of the *Hin*dIII site. The sequence of the *Nco*I-*Hin*dIII fragment in pCO12R was verified (data not shown). The entire *coo*-insert region was subsequently excised by *Pvu*II digestion and ligated to the mobilizable vector pUX19 (Km^r) cut with *Hin*cII. This construct, in *E. coli* S17-1 (UQ324[25]), was mated into *R. rubrum* UR485 (Δ*cooS::aacC1*Ω). The isolated *R. rubrum* Km^rGm^r merodiploid recombinant was designated UR502.

**Cell Growth and Protein Purification.** Strain UR502 (C531A CODH) was cultured in medium which was, depending upon the experiment, either completely lacking nickel or supplemented with 0.05 mM NiCl₂, according to established procedures.[26] All buffers used for culture growth were passed through a metal-chelating column of Bio-Rad Chelex-100 cation-exchange resin before the addition of the necessary metals, as were all buffers used in protein purification. Metal-free 100 mM MOPS buffer was used both in protein purification and in assays of C531A CODH activity. Holo- (Ni-containing) and Ni-deficient C531A CODH were purified as described previously for the wild-type enzyme.[1,20,26,27]

(12) Hu, Z.; Spangler, N. J.; Anderson, M. E.; Xia, J.; Ludden, P. W.; Lindahl, P. A.; Münck, E. *J. Am. Chem. Soc.* **1996**, *118*, 830−845.

(13) Anderson, M. E.; Lindahl, P. A. *Biochemistry* **1994**, *33*, 8702−8711.

(14) DeRose, V. J.; Telser, J.; Anderson, M. E.; Lindahl, P. A.; Hoffman, B. M. *J. Am. Chem. Soc.* **1998**, *120*, 8767−87776.

(15) Beinert, H.; Kennedy, M. C.; Stoudt, C. D. *Chem. Rev.* **1996**, *96*, 2335−2373.

(16) Bastian, N. R.; Diekert, G.; Niederhoffer, E. C.; Teo, B.-K.; Walsh, C. T.; Orme-Johnson, W. H. *J. Am. Chem. Soc.* **1988**, *110*, 5581−5582.

(17) Xia, J. Q.; Dong, J.; Wang, S. K.; Scott, R. A.; Lindahl, P. A. *J. Am. Chem. Soc.* **1995**, *117*, 7065−7070.

(18) Spangler, N. J.; Lindahl, P. A.; Bandarian, V.; Ludden, P. W. *J. Biol. Chem.* **1996**, *271*, 7973−7977.

(19) Xia, J. Q.; Lindahl, P. A. *J. Am. Chem. Soc.* **1996**, *118*, 483−484.

(20) Ensign, S. A.; Campbell, M. J.; Ludden, P. W. *Biochemistry* **1990**, *29*, 2162−2168.

(21) Volbeda, A.; Charon, M.-H.; Piras, C.; Hatchikian, E. C.; Frey, M.; J. C., F.-C. *Nature* **1995**, *373*, 580−587.

(22) Deng, W. P.; Nickoloff, J. A. *Anal. Biochem.* **1992**, *200*, 81−88.

(23) Zhang, Y.; Burris, R. H.; Ludden, P. W.; Roberts, G. P. *J. Bacteriol.* **1996**, *178*, 2948−2953.

(24) Kerby, R. L.; Ludden, P. W.; Roberts, G. P. *J. Bacteriol.* **1997**, *179*, 2259−2266.

(25) Simon, R.; Priefer, U.; Pahler, A. *Biotechnology* **1983**, *1*, 784−791.

(26) Bonam, D.; McKenna, M. C.; Stephens, P. J.; Ludden, P. W. *Proc. Natl. Acad. Sci. U.S.A.* **1988**, *85*, 31−35.

(27) Ensign, S. A.; Bonam, D.; Ludden, P. W. *Biochemistry* **1989**, *28*, 4968−4973.

**CODH Activity Assays.** The activity of C531A CODH was determined by its ability to reduce methyl viologen when in the presence of CO.[27] The $K_m$ for methyl viologen was measured by a manner identical to that of the activity assay but at varying concentrations of methyl viologen.

**Metal Analysis.** Determination of the metal content of the enzyme solutions was performed at the University of Georgia by inductively coupled plasma mass spectrometry (ICP-MS). Enzyme samples were desalted by a $0.5 \times 10$ cm Sephadex G-25 column equilibrated in 10 mM MOPS buffer at pH 7.5 before shipment for metal analysis. Metal atoms/monomer were calculated using the ICP-MS results in conjunction with the protein assays described below.

**Protein Assays.** The CODH samples were determined from SDS and native PAGE analysis to be greater than 99% pure. Total protein concentration was determined for each sample described in this study from 10 replicate protein assays using 2 and 5 $\mu$L of CODH solution per milliliter of assay solution and a 3-replicate standard curve of 0−50 $\mu$g/mL in 2 $\mu$g/mL increments. Protein assays were performed in the absence of sodium dithionite.

**Preparation of Samples for UV−Vis Spectroscopy.** All manipulations were performed in an anaerobic glovebox (Vacuum Atmospheres) under an atmosphere containing less than 2 ppm $O_2$. Purified CODH, either wild-type or C531A, in buffer containing 2 mM dithionite was passed down a Sephadex G-25 column equilibrated in 100 mM MOPS buffer at pH 7.5 to remove excess dithionite. For preparation of CODH in the oxidized or partially reduced states, the enzyme was then treated with an excess of thionin ($E_m = +64$ mV versus SHE) or 95% reduced indigo carmine (indigo disulfonate, $E_m = -125$ mV versus SHE at pH 7.0), respectively. Indigo carmine was determined to be 95% reduced by monitoring the absorption and titrating with ultrapure sodium dithionite. The dyes and salt were subsequently removed from CODH by passage of the enzyme through a $0.5 \times 10$ cm Sephadex G-25 column equilibrated with 100 mM MOPS buffer pH 7.5. The oxidized CODH solution was transferred to quartz cuvettes, which were sealed with rubber serum stoppers before bringing the samples out of the glovebox for UV−vis spectral measurements. Enzyme pretreated with either dye was subsequently titrated with a 1 mM sodium dithionite solution until the first appearance of the characteristic dithionite absorption at 314 nm. The dithionite solution was added by gastight syringe through the serum stopper. Spectra were also recorded for samples treated with a large excess of dithionite to ensure that all species reducible by dithionite were fully reduced. Where indicated, CO was introduced with a gastight syringe into the headspace of stoppered quartz cuvettes containing CODH. The CODH was incubated under CO at room temperature for 5 min, and the spectrum was recorded. Identical samples were prepared for electron paramagnetic resonance (EPR) spectroscopic analysis. Molar absorption coefficients of wild-type and C531A CODH were obtained from the absorption spectra and the protein assays described above.

**Preparation of Samples for EPR.** All manipulations were performed in an anaerobic glovebox (Vacuum Atmospheres) under an atmosphere of less than 2 ppm $O_2$. Purified C531A CODH in buffer containing 2 mM dithionite was passed down a Sephadex G-25 column equilibrated in 10 mM MOPS buffer at pH 7.5 to remove excess dithionite. Most protein concentrations were 10 mg/mL. For indigo carmine- or thionin-poised samples, dye was added until the color of oxidized dye persisted. For dithionite-treated samples, sodium dithionite was added to a final concentration of 1 mM. For CO-treated samples, CO was introduced into the headspace of a stoppered vial containing the enzyme with a very slight excess of either thionin or indigo carmine and allowed to equilibrate with the enzyme solution for the length of time indicated in the Results section. For CN⁻-treated samples, a sample of freshly prepared, anaerobic KCN solution was added to a stoppered vial containing the CODH to yield the final CN⁻ concentration indicated in the Results section.

**UV−Vis and EPR Spectroscopy.** UV−Vis spectra of samples anaerobically sealed in quartz cuvettes were recorded using a Shimadzu UV-1601PC spectrophotometer. Perpendicular-mode X-band electron paramagnetic resonance (EPR) spectra were recorded in the laboratory of Professor George Reed using a Varian E-15 EPR spectrometer equipped with a Hewlett-Packard 5255A frequency counter, a Varian

**Table 1.** Metal Content and Kinetics Constants for C531A and Wild-type CODH

|  | C531A | wild-type |
|---|---|---|
| metal content (mol of metal/mol of enzyme) | | |
| Ni | $0.85 \pm 0.05$ | $0.97 \pm 0.09$ |
| Fe | $8.9 \pm 0.3$ | $8.9 \pm 0.3$ |
| kinetics constants | | |
| CO oxidation | | |
| $V_{max}$ (units/mg) | 4.22 | 7700[a] |
| $K_{m\,CO}$ ($\mu$M) | 11.40 | 32[a] |
| $k_{cat}/K_{m\,CO}$ ($S^{1-}M^{-1}) \times 10^6$ | 0.41 | 250[a] |
| $K_{m\,MV}$ (mM)[b] | 3.8 | 3.1[a] |
| CN⁻ interaction | | |
| $K_{D,\,CN}$ ($\mu$M, by monitoring activity) | 46.55 | 8.46 |
| "$K_{D,CN}$" (mM, by monitoring absorbtion) | nd[c] | $0.75 \pm 0.34$ |

[a] Previously published data.[27,45]  [b] MV, methyl viologen. [c] Not determinable due to enzyme denaturation.

E102 microwave bridge, an Oxford Instruments ER910A cryostat, and an Oxford 3120 temperature controller. The microwave frequency was 9.23 GHz. EPR quantitations were carried out under nonsaturating conditions using 1 mM CuEDTA as the standard.

**Materials.** Reagent grade (99.9%) Tris(hydroxymethyl)aminomethane (Tris), NaCl, and sodium phosphate ($Na_3PO_4$) were obtained from Fisher Scientific. 3-(N-Morpholino)propanesulfonic acid (MOPS) was obtained from Amersham Life Sciences. Sephadex G-25 was obtained from Pharmacia Biotech. Hydroxylapatite (fast flow) was obtained from Calbiochem. Chelex 100 resin (50−100 mesh, sodium form) was obtained from Bio-Rad. DEAE cellulose (DE-52) was obtained from Whatman. Indigo carmine and potassium cyanide (97.8%) were obtained from Sigma. Thionin (86%) was obtained from Aldrich. CO (99.5%) was obtained from AGA Gas, Inc. $^{13}$CO was obtained from Isotec, Inc. $^{61}$Ni was obtained from Oakridge National Laboratory. $^{57}$Fe was obtained from Pennwood Chemicals, Inc. Sodium dithionite (hydrosulfite) (85%) was obtained from Fluka and contains approximately 15% sodium bicarbonate. Ultrapure dithionite (bicarbonate-free) was obtained in a sealed ampule as a gift from Dr. R. H. Burris.
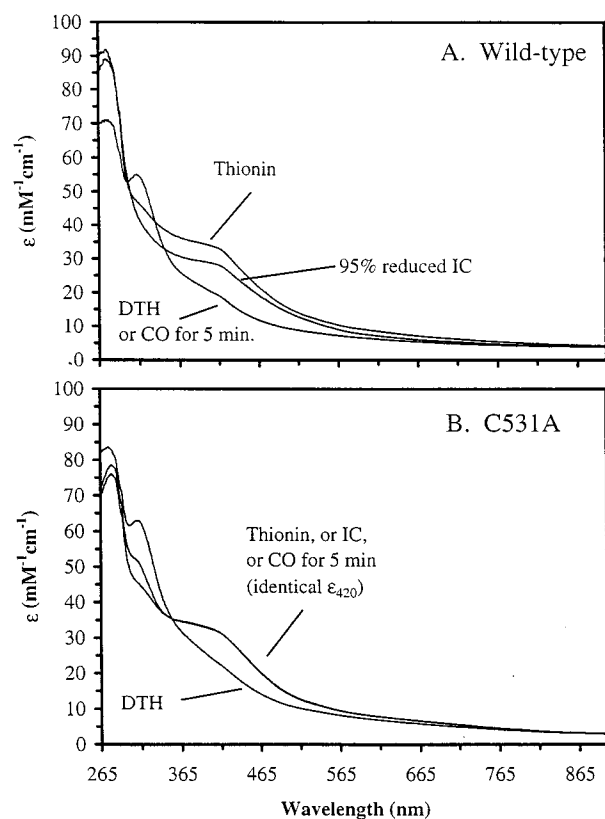
## Results

**Metal Content, Activity, and Kinetic Data.** C531A CODH was purified according to the published protocol for wild-type CODH with a similar yield. Although the specific activity of C531A CODH is much lower than that of wild-type CODH, the percent yield of activity was comparable throughout the purification protocol. Wild-type and C531A CODH have a nearly identical metal content, indicating that C531A CODH contains similar compositions of iron−sulfur clusters and of Ni (Table 1). The iron content in every sample (C531A or wild-type) of CODH tested using the protein analysis methods described in Experimental Procedures is close to 9 Fe atoms/ monomer CODH. Analyses represent the average of 3 (C531A CODH) and 20 (wild-type CODH) independent determinations. Protein assays were repeated 10 times and were standardized to pure carbonic anhydrase; carbonic anhydrase standards were confirmed using the known extinction coefficient for the protein at 280 nm. Previous estimates of the Fe content of the enzyme have shown 7−9 atoms of Fe/monomer of CODH. The very low rate of CO oxidation catalyzed by C531A CODH (0.05% of wild-type) is consistent with data that will be presented later, which suggests that either the ligation of one cluster is changed or that the interaction between clusters is perturbed. Table 1 also shows that the $K_m$ for the electron-accepting dye (methyl viologen) is relatively unchanged and the $K_m$ for CO is actually lower than that of the wild-type CODH. Therefore, the low activity is not due to an inability of C531A CODH to interact with CO or to interact with the electron acceptor. The slow

turnover of C531A CODH suggests that cys-531 is directly involved in the catalytic site of CODH.

Cyanide (CN⁻) is a slow, tight binding, competitive inhibitor of *R. rubrum* CODH.[28] The $K_D$ for CN⁻ of C531A CODH using a protein concentration of 100 $\mu$M was measured by activity assay to be 46.55 $\mu$M. This value is higher than the 8.46 $\mu$M reported for wild-type CODH.[28] The apparent difference in $K_D$ for CN⁻ obtained by monitoring activity may reflect the fact that very high protein concentrations of C531A CODH were needed to achieve measurable initial activity readings, even in the absence of CN⁻. When CN⁻ was added, the concentration of C531A CODH actually exceeded that of CN⁻. The method reported for obtaining a "$K_D$" for SCN⁻ for *C. thermoaceticum* CODH by monitoring changes in absorption [11] was attempted for wild-type *R. rubrum* CODH (0.021 mM). A value of 0.75 ± 0.34 mM [CN⁻] was obtained using this method. However, as will be discussed later, addition of high concentrations of CN⁻ (5−10 mM) to wild-type *R. rubrum* CODH results in *irreversible* inactivation, suggesting that the measured value is not a "$K_D$". High concentrations of CN⁻ (5−10 mM) cause changes in the absorption spectrum of CODH. Attempts were made to measure $k_1$ for the inactivation process by monitoring changes in absorption as a function of time; however, the inactivation rate could not be accurately measured. Additions of concentrations of CN⁻ (5−10 mM), which produce the changes in absorption in wild-type CODH, result in the denaturation of C531A CODH.

**UV−Vis Spectroscopy.** To determine the redox states of the [Fe₄S₄] clusters of C531A CODH at several potentials, the UV−vis spectra of the protein were determined using defined redox conditions and were compared to the spectra of wild-type CODH under identical conditions. As shown in Figure 1, spectra were recorded for wild-type (Figure 1A) and C531A (Figure 1B) CODHs (i) oxidized with thionin, (ii) poised with 95% reduced indigo carmine, (iii) reduced with dithionite, and (iv) treated with CO. The values of $\epsilon_{420}$ for thionin-oxidized C531A and wild-type CODH are very similar, suggesting that C531A has a full complement of [Fe₄S₄] clusters. Both dithionite and CO rapidly reduce the wild-type enzyme (Figure 1A) in agreement with published data. In contrast, the [Fe₄S₄] clusters of C531A CODH are rapidly reduced by dithionite but not by CO. Over the course of several hours a slow reduction of the [Fe₄S₄] clusters of C531A CODH was observed upon treatment with CO, in accordance with its very low catalytic rate (data not shown). The [Fe₄S₄] clusters have not received reducing equivalents upon treatment with CO in C531A CODH on the time scale which produces full reduction of the [Fe₄S₄] clusters in wild-type CODH, although they have received reducing equivalents when treated with dithionite. Therefore, C531A CODH is unable to transfer electrons from the site of CO oxidation to [Fe₄S₄]_C. These results suggest one or more of the following: (i) that the site of CO binding is nonfunctional in CO oxidizing; (ii) that [Fe₄S₄]_C is nonfunctional in accepting electrons from the site of CO oxidation; (iii) that the site of CO oxidation is nonfunctional in donating electrons to [Fe₄S₄]_C; or (iv) that a conduit of electron flow between the two sites is interrupted. Implicit in these possibilities is the assumption that the site of CO oxidation is not [Fe₄S₄]_C. This assumption will later be substantiated by EPR data.

Treatment of thionin-oxidized ($E_m$ = +64 mV versus SHE; approximate $E$ = +128 mV when 100% oxidized) C531A CODH with 95% reduced indigo carmine ($E_m$ = −140 mV versus SHE at pH 7.5; calculated $E$ = −178 mV) resulted in



**Figure 1.** UV−vis absorption spectra of as-purified (CODH is purified in buffer containing 2 mM sodium dithionite.) wild-type (34.0 $\mu$M) and C531A (15.6 $\mu$M) CODH oxidized with thionin and subsequently treated with 95% reduced indigo carmine (IC), CO, or dithionite (DTH): (A) wild-type CODH, (B) C531A CODH.
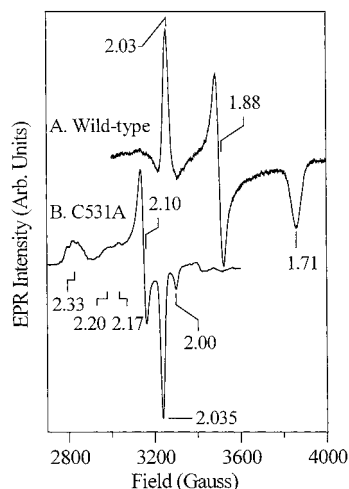
no change in the molar extinction coefficient at 420 nm ($\epsilon_{420}$) from that of thionin-treated C531A CODH (Figure 1B). This is markedly different from wild-type CODH (Figure 1A), where addition of 95% reduced indigo carmine to the oxidized enzyme resulted in a decrease of $\epsilon_{420}$. The decrease in $\epsilon_{420}$ observed for wild-type CODH equates to 50% of the decrease in $\epsilon_{420}$ observed upon dithionite treatment (Figure 1A). This result, in conjunction with EPR data presented below, indicates that one [Fe₄S₄] cluster (we will show that it is [Fe₄S₄]_C) is fully reduced while the other ([Fe₄S₄]_B) remains in the oxidized state. As described below, the fact that both [Fe₄S₄] clusters in C531A CODH remain oxidized upon treatment with indigo carmine is very important in the interpretation of the EPR spectra of this enzyme variant.

**EPR Spectroscopy. a. Indigo Carmine Poising.** Wild-type CODH exhibits an EPR signal with apparent *g* values of $g_{z,y,x}$ = 2.03, 1.86, and 1.71 reported in apparent low-spin concentration (0.10−0.60 spins/molecule) when the reduced enzyme is oxidized with methyl viologen or poised near −160 mV with indigo carmine (Figure 2).[18] This feature has been referred to as C_red1 and has been believed to arise from the weak exchange-coupling of high-spin ($S$ = 1, EPR unobservable) Ni²⁺ with a reduced ($S$ = ¹/₂) [Fe₄S₄]¹⁺ cluster, perturbing the spectrum of the cluster.[12] This interpretation was based upon the observation that the line widths of the EPR spectrum of C_red1 are variably broadened by both ⁶¹Ni and ⁵⁷Fe,[12,29,30] as well as the observation of anomalous iron site in the Mössbauer spectrum, which suggested that one iron of an [Fe₄S₄] cube has

(28) Ensign, S. A.; Hyman, M. R.; Ludden, P. W. *Biochemistry* **1989**, *28*, 4973−4979.

(29) Ragsdale, S. W.; Wood, H. G. *J. Biol. Chem.* **1985**, *260*, 3970−3977.

(30) Stephens, P. J.; McKenna, M.-C.; Ensign, S. A.; Bonam, D.; Ludden, P. W. *J. Biol. Chem.* **1989**, *264*, 16347−16350.
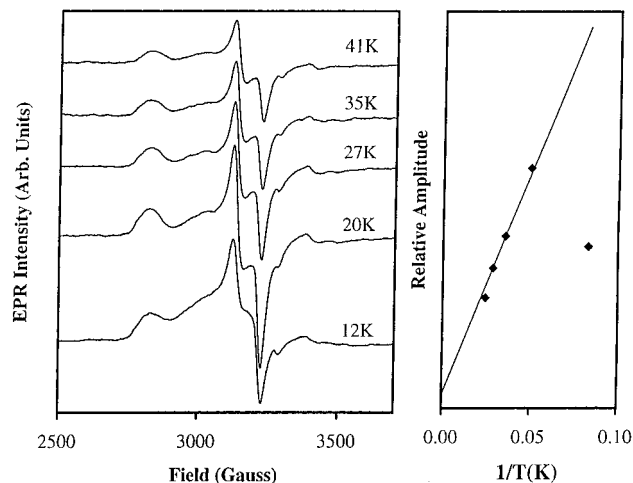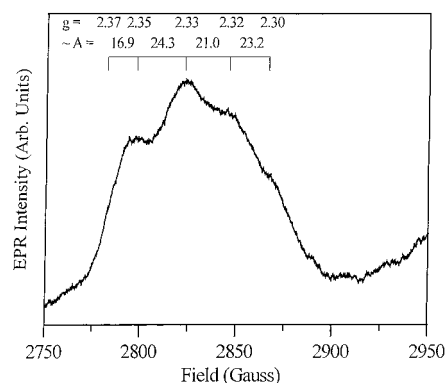
**Figure 2.** EPR spectra of wild-type (0.15 mM) and C531A (0.15 mM) CODH poised with 95% reduced indigo carmine (−178 mV versus SHE). (A) Wild-type CODH: temperature = 10.0 K, microwave power = 1.0 mW, modulation amplitude = 10 G. (B) C531A CODH: 20 K and 0.16 mW, modulation amplitude = 4 G.



**Figure 3.** Behavior as a function of temperature of the EPR spectrum of C531A CODH (0.15 mM) poised with 95% reduced indigo carmine. Left panel: EPR spectra taken at 0.16 mW. Right panel: Total spin intensity of the spectra shown in the left panel plotted versus reciprocal temperature in Kelvin. Modulation amplitude = 10 G.
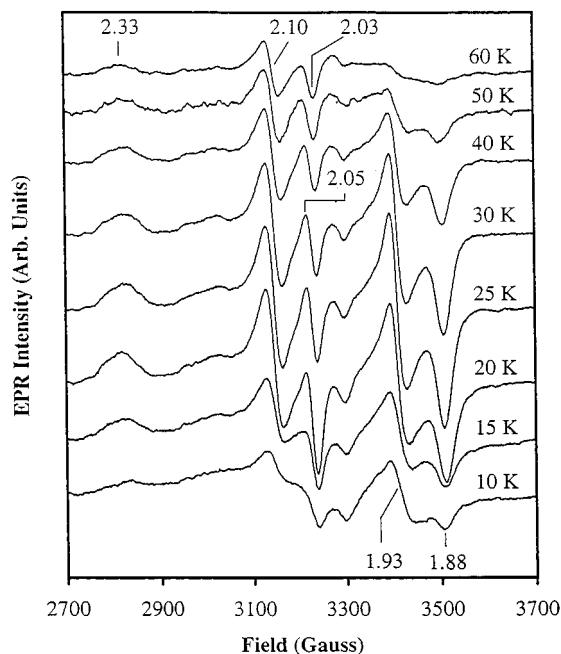
unusual coordination.[10,12] Redox titrations show a midpoint potential of approximately −110 mV versus SHE for the appearance of the $C_{red1}$ signal.[18,31] Treatment of oxidized C531A CODH with 95% reduced indigo carmine, or titration of CO-treated C531A CODH with oxidized indigo carmine until a slight color of oxidized indigo carmine persists, results in a signal with a very broad resonance at $g = 2.33$ and other resonances at $g = 2.10$, 2.05, and 2.01 ($g_{ave} \cong 2.16$, Figure 2), quantifying maximally to $0.90 \pm 0.10$ spin/molecule of enzyme. $C_{red1}$ is not observed in the EPR spectrum of C531A CODH. The $g_{ave} = 2.16$ feature is similar to that observed in azide-treated *C. thermoaceticum* CODH[32] but with much better resolution. Additional resonances are observed at $g = 2.20$, 2.17, and 2.00 (Figure 2), the importance of which will be discussed below. Studies of the effect of temperature (Figure 3) at the nonsaturating power of 0.16 mW reveal that the optimum temperature for observation of an undistorted signal is approximately 20 K. At conditions of lower temperature and higher power, the line shapes of the resonances are extremely distorted due to power saturation effects, displaying a featureless rise from $g = 2.35$ to 2.10 and a derivative shape at $g = 2.07$. In Figure 4 the apparent $g_z = 2.33$ feature is further characterized using optimum conditions (20 K, 0.16 mW), with a small modulation amplitude (4 G). Fine structure is readily observed under these conditions, indicating that the $g = 2.33$ feature is actually either a combination of several slightly different absorbing species with this as their most differing $g$ value and/or that nuclear superhyperfine from atom(s) with a nonzero nuclear spin (e.g., $^{14}N$) is causing a splitting of the resonance. We prefer the latter explanation for reasons which will be discussed later. The $g_{ave} = 2.16$ resonance of $^{61}$Ni-grown C531A CODH is not detectably broadened by the $^{61}$Ni nuclear spin ($I = ^3/_2$), indicating that no significant unpaired spin density resides on the Ni atom.

**b. CO Reduction.** Treatment of C531A CODH with CO for 1 h (Figure 5) resulted in the appearance of an EPR spectrum, which consisted of the combination of small spin quantities of

(31) Ludden, P. W.; Roberts, G. P.; Kerby, R. L.; Spangler, N.; Fox, J.; Shelver, D.; He, Y.; Watt, R. *The biochemistry of CO dehydrogenase in Rhodospirillum rubrum*; Lidstrom, M. E., Tabita, F. R., Eds.; Kluwer Academic: San Diego, CA, 1996; pp 183−190.

(32) Kumar, M.; Lu, W.-P.; Smith, A.; Ragsdale, S. W.; McCracken, J. *J. Am. Chem. Soc.* **1995**, *117*, 2939−2940.

**Figure 4.** Expansion of the $g = 2.33$ region of the $g_{ave} = 2.16$ resonance of C531A CODH taken at 20.0 K, and 0.16 mW, with a modulation amplitude of 4.0 G. Approximate distances between hyperfine lines are shown as ~A (approximate hyperfine coupling constants). Sample is as described in Figure 2B.

the $g_{ave} = 2.16$ signal and another signal. The normalized EPR spectrum of the $g_{ave} = 2.16$ signal can be subtracted from the EPR spectrum of C531A CODH treated with CO for 1 h to yield a largely undistorted spectrum of a slow-relaxing $[Fe_4S_4]^{1+}$ component with $g$ values of 2.04, 1.93, and 1.89 (subtraction not shown), indicating that these two paramagnetic species are largely not spin-interacting. The total spin intensity of both signals combined was $0.20 \pm 0.05$ spins/molecule at 1 h incubation, but the total spin intensity was dependent upon the duration of incubation with CO. The $[Fe_4S_4]^{1+}$ cluster is slow-relaxing, as it is observable to 50 K and is power saturated at low temperatures. It displays different relaxation properties from those normally attributed to the fast-relaxing $[Fe_4S_4]_B^{1+}$ and is thus assigned to $[Fe_4S_4]_C^{1+}$ that is not coupled to another spin system. There are no traces of the spectroscopic features referred to as $C_{red1}$ ($g_x = 1.71$) or $C_{red2}$ ($g_x = 1.75$).
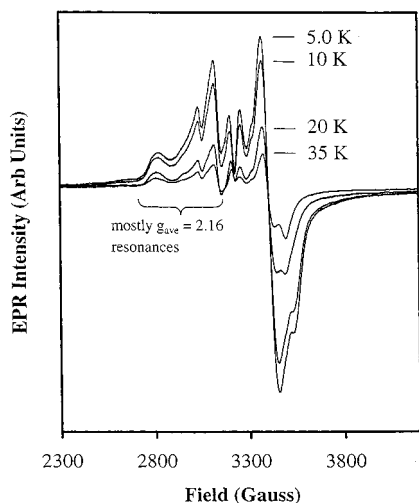
**c. Dithionite Treatment.** Treatment of C531A with dithionite results in a complex spectrum that consists of signals arising from two reduced $[Fe_4S_4]$ clusters, as is evident by the temperature dependence of the resonances (Figure 6), in addition to the $g_{ave} = 2.16$ signal described above. The fast-relaxing resonance characteristic of $[Fe_4S_4]_B^{1+}$ overlays the slow-relaxing cluster shown in Figure 5. The spectrum taken at 35 K nearly overlays the normalized spectrum of C531A CODH treated with
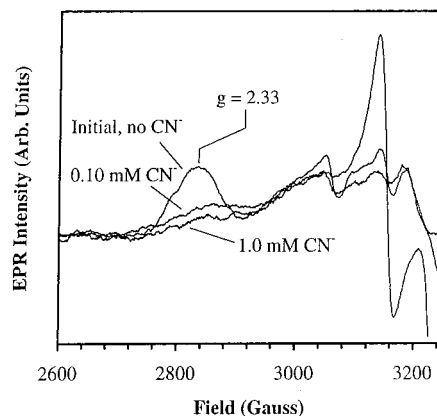
**Figure 5.** Temperature dependence of the EPR spectrum of thionin-oxidized C531A (0.15 mM) subsequently incubated with CO for 1 h. Temperatures as indicated; microwave power = 1.0 mW; modulation amplitude = 12.5 G.



**Figure 6.** Temperature dependence of the EPR spectrum of dithionite-treated C531A CODH (0.15 mM). Temperatures are 5.0, 10.0, 20.0, and 35.0 K. Microwave power = 0.16 mW; modulation amplitude = 12.5 G.
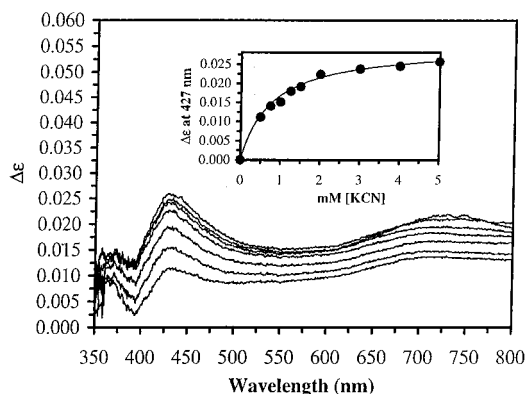
CO for 1 h (not shown), indicating that the two slow-relaxing species in dithionite-treated C531A CODH are identical to the slow-relaxing species observed upon CO-treatment of C531A CODH. In agreement with the spectral features and the molar extinction coefficients, the maximum total $g = 2$ spin quantifies to $2.80 \pm 0.10$ spins/molecule of C531A CODH under non-power-saturating conditions (0.16 mW). C531A CODH treated with dithionite also shows no trace of either $C_{red1}$ or $C_{red2}$. Subtraction of the $g_{ave} = 2.16$ signal alone from the dithionite-treated sample, or subtraction of the normalized spectrum of the CO-treated sample (see Figure 5) from the spectrum of the dithionite-treated sample, does not yield a simple spectrum for what would be assumed to be $[Fe_4S_4]_B{}^{1+}$ (data not shown). This indicates that the spin of $[Fe_4S_4]_B{}^{1+}$ weakly interacts with another paramagnetic species. The $g = 2.33$ resonance doubles in amplitude in going from 20 to 10 K in dithionite-treated



**Figure 7.** Effect of micromolar and millimolar amounts of KCN on the EPR spectra of C531A CODH pre-poised with 95% reduced indigo carmine. EPR conditions: temperature = 20.0 K, microwave power = 1.0 mW, modulation amplitude = 12.5. $CN^-$ incubation time was 30 min before freezing. Enzyme concentration was 0.10 mM, the same concentration as those used to determine $K_{D,CN}$ by monitoring enzyme activity.

samples (Figure 6) but virtually disappears due to saturation during the same temperature drop when $[Fe_4S_4]_B{}^{1+}$ is not present (Figure 5). Therefore, it is possible that $[Fe_4S_4]_B{}^{1+}$ weakly interacts with the 2.16 signal.

**d. Cyanide Treatment.** Cyanide is a slow, tight-binding inhibitor of CODH. The effect of $CN^-$ on the $g_{ave} = 2.16$ signal of C531A CODH was tested and found to be significant. Indigo carmine-poised C531A CODH, which had been pretreated with CO, was divided into three equal fractions. The first fraction gave the characteristic $g_{ave} = 2.16$ resonance shown in Figure 2B (Figure 7). Incubation of the second fraction for 30 min with 0.10 mM $CN^-$ resulted in the almost complete loss of the $g_{ave} = 2.16$ resonance (Figure 7). Incubation of the third fraction for 30 min with 1.0 mM $CN^-$ did not result in any additional significant changes in the EPR spectral line shape but a 14.6% further reduction in the intensity of the feature centered at $g = 2.33$ (and similar decreases in the other $g$ values). The 0.10 and 1.0 mM $CN^-$ concentrations were chosen on the basis of the concentrations of $CN^-$, which did not or did produce significant changes in the UV−vis absorption spectrum in wild-type CODH, respectively. An apparent dissociation constant, "$K_D$", for $CN^-$ obtained by monitoring changes in the molar extinction coefficient at 427 nm of wild-type CODH at an enzyme concentration of 0.020 mM was $0.75 \pm 0.34$ mM $[CN^-]$ (as shown in Figure 8, inset). The method is similar to that previously reported in the literature for *C. thermoaceticum* CODH using $SCN^-$;[11] however, "$K_D$" is an incorrect term for the process using $CN^-$ with *R. rubrum* CODH because, as discussed below, the enzyme is irreversibly inactivated at these concentrations. The measured $K_{D,CN}$ determined by monitoring CO oxidation activity using a 0.75 nM solution of wild-type CODH was 8.46 $\mu$M $[KCN]$.[28] Wild-type CODH, which experienced changes in molar extinction coefficient (thus high $[CN^-]$), could not regain activity upon removal of excess $CN^-$; however, those samples treated with lower concentrations (100 $\mu$M or less) of $CN^-$ regained 90% of their initial activity upon removal of excess $CN^-$ and subsequent preincubation with CO. This result indicates that there are at least two distinct interaction sites for $CN^-$. The interaction of $CN^-$ at one site only results in reversible enzyme inactivation, whereas the interaction of $CN^-$ at the other site produces changes in the molar extinction coefficient. These changes in molar extinction coefficient are concurrent with partial denaturation of the enzyme, based upon
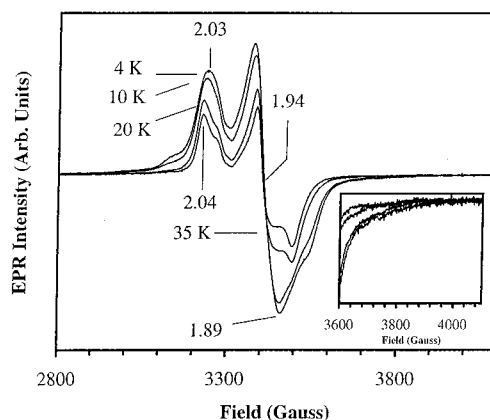
**Figure 8.** Effect of millimolar amounts of KCN on the UV−vis spectra dithionite-treated wild-type CODH. $K_{D,CN}$ for the irreversible inactivation is shown using an enzyme concentration of 0.021 mM, with a reference wavelength of 427 nm. KCN was added to final concentrations of 0.50, 0.75, 1.00, 1.25, 1.50, 2.00, 3.00, 4.00, and 5.00 mM.

the appearance of cloudiness in the sample and the overall increase in absorbance across the entire spectral range. Therefore, a "$K_D$" determined by this method is invalid for the *R. rubrum* enzyme.

Because observation of the $g_{ave} = 2.16$ species does not require a concurrent change in the UV−vis spectrum, low concentrations of CN⁻ that did not cause changes in the UV−vis spectrum at 420 nm were chosen to see if the loss of activity of C531A CODH could be correlated with a change in the $g_{ave} = 2.16$ species. This would indicate that one site of CN⁻ interaction is the site giving rise to the $g_{ave} = 2.16$ species. Identical concentrations of enzyme were used for $K_{D,CN}$ (CO oxidation activity) and EPR measurements of C531A CODH, so inhibitory effects could be directly correlated to spectroscopic changes. This was only possible because of the exceptionally slow turnover rate of the enzyme. At 0.10 mM [CN⁻], the enzyme is measured to be 78% inhibited by activity assay. This value is similar to the observed 85.4% decrease in intensity of the $g = 2.33$ feature of the $g_{ave} = 2.16$ species at 0.10 mM [CN⁻], referenced against intensity of the $g = 2.33$ feature of C531A CODH with a 1.0 mM CN⁻ concentration (see Figure 7), which was determined to be the concentration of 100% inhibition by activity assays. Thus, a decrease in the $g_{ave} = 2.16$ species parallels the loss of activity of C531A CODH. The $g_{ave} = 2.16$ signal can be regained after removal of micromolar concentrations of CN⁻ by a procedure that involves passing the enzyme down a Sephadex G25 column, treatment with CO, removal of excess CO by repeated vacuum-flush, and rapid repoising with indigo carmine (data not shown). Ninety percent of the initial activity can also be regained in this manner in C531A. In contrast, no enzyme activity can be regained after treatment with 5 mM [CN⁻].

A concentration of CN⁻ greater than 1.0 mM destroys enzyme activity permanently in wild-type CODH and also results in a change in absorption of the enzyme. Changes in absorption on the scale observed can only be caused by changes in the [Fe₄S₄] species. In contrast, the inhibitory effects of micromolar amounts of CN⁻ are completely reversed in wild-type CODH by CO treatment. The studies presented here and in the accompanying articles show that [Fe₄S₄]$_C$ has unusual relaxation properties that are inconsistent with an all-cysteinyl liganded cluster. It is possible, on the basis of UV−vis spectroscopic studies, that [Fe₄S₄]$_C$ irreversibly binds a CN⁻ molecule at a site of noncysteinyl ligation, resulting in complete enzyme inactivation. It is also possible that CN⁻ causes the breakdown of [Fe₄S₄]$_C$, which in turn causes the partial denaturation of CODH.



**Figure 9.** Temperature dependence of the EPR spectrum of dithionite-treated Ni-deficient C531A CODH (0.10 mM). Temperatures are 4.0, 10.0, 20.0, and 35.0 K. EPR conditions: microwave power = 1.0 mW; modulation amplitude = 12.5 G.

Therefore, these results indicate that the high "$K_D$" for CN⁻ obtained by monitoring changes in the UV−vis spectrum reflects the interaction of CN⁻ with [Fe₄S₄]$_C$ rather than with the [FeNi] cluster.

**e. Dithionite Treatment of Ni-Deficient C531A CODH.** Figure 9 shows the EPR spectrum of Ni-deficient C531A CODH obtained from cells of strain UR502 grown in the absence of Ni. It exhibits only resonances arising from two reduced iron−sulfur clusters, the first being the slow-relaxing [Fe₄S₄]$^{1+}$ cluster that is observed at temperatures up to 50 K in both dithionite-treated wild-type CODH and dithionite-treated C531A CODH (see Figure 6). This signal is also observed in CO-treated C531A CODH (see Figure 5). The second cluster is faster-relaxing with properties more like all-cysteinyl liganded clusters. [Fe₄S₄]$_B^{1+}$ has been described as a typical all-cysteinyl liganded cluster; therefore, the fast-relaxing cluster is assigned to [Fe₄S₄]$_B^{1+}$ and the slow-relaxing cluster is assigned to [Fe₄S₄]$_C^{1+}$. The spectrum of dithionite-treated Ni-deficient C531A CODH is identical to that of dithionite-treated Ni-deficient wild-type CODH. Spin quantitations of the $g = 2$ region of dithionite-treated C531A CODH yield a value of 1.70 ± 0.10, a value not equal to 2.0 because of the presence of an $S = {}^3/_2$ form of [Fe₄S₄]$_C^{1+}$ (data not shown), also observed in wild-type CODH. The Ni-deficient form of C531A CODH lacks the $g_{ave} = 2.16$ EPR signal in the dithionite-reduced state (Figure 9) and at all other potentials (data not shown).

**Discussion**
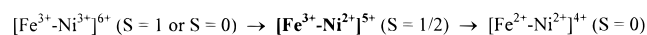
**The $g_{ave} = 2.16$ Signal Cannot Be Attributed to Any Known Metal Cluster in *R. rubrum* CODH.** A metal cluster that cannot be attributed to [Fe₄S₄]$_C$ or [Fe₄S₄]$_B$ is observed in indigo carmine-poised C531A CODH (Figures 2 and 3). This metal cluster is attributed to a [FeNi] cluster. Thionin-oxidized ($E_{m,pH\ 7.5} = +64$ mV versus SHE, approximate $E = +128$ mV) C531A CODH exhibits no observable EPR spectrum, while CO-pretreated C531A CODH poised with 95% reduced indigo carmine ($E_{m,pH\ 7.5} = -140$ mV versus SHE) displays an EPR spectrum ($g_{z,y,x} = 2.33, 2.16, 2.04; g_{ave} = 2.16$) in the $S = {}^1/_2$ region with a maximal spin quantity of 0.90 spins/molecule. However, the redox event responsible for the production of the $g_{ave} = 2.16$ species does not involve the reduction of an [Fe₄S₄] cluster because the molar extinction coefficient at 420 nm ($\epsilon_{420}$) is identical upon treatment with either dye, indicating that both of the known [Fe₄S₄] clusters are in the oxidized [Fe₄S₄]$^{2+}$ ($S = 0$) state. Other than iron, the only metal known to be

present in the enzyme is nickel. Because nickel typically has very small molar extinction coefficients, assignment of the $g_{ave} = 2.16$ species to paramagnetic Ni seemed a plausible explanation for the origin of the $g_{ave} = 2.16$ signal. However, C531A CODH grown on $^{61}Ni$ has a $g_{ave} = 2.16$ resonance with spectral line widths identical to those of C531A CODH grown on natural abundance nickel. Therefore, the $g_{ave} = 2.16$ species does not arise from paramagnetic Ni and no significant unpaired spin density resides upon Ni, suggesting that Ni is diamagnetic ($S = 0$). A nearly identical $g_{ave} = 2.16$ species has been produced in *C. thermoaceticum* CODH/ACS when the reduced enzyme was treated with various inhibitors, including azide,[32] thiocyanate, and cyanate.[11] In all cases, a lack of hyperfine broadening arising from $^{61}Ni$ ($I = 3/2$) was reported. However, broadening of the $g_{ave} = 2.16$ species that resulted from azide treatment was reported for the $^{57}Fe$-substituted enzyme.[32]

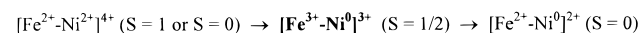Attempts have been made to explain the unusual $g_{ave} = 2.16$ species in *C. thermoaceticum* as arising from $[Fe_4S_4]_C^{1+}$ weakly spin-coupling with $Ni^{2+}$ ($S = 1$).[12] While this interpretation explains the lack of significant broadening by $^{61}Ni$, it is inconsistent with the observation that the production of the $g_{ave} = 2.16$ signal in C531A CODH occurs without a concurrent change in $\epsilon_{420}$ (Figures 1 and 2). Furthermore, reduction of $[Fe_4S_4]_C$ and $[Fe_4S_4]_B$ can be observed to produce significantly different EPR spectra from the $g_{ave} = 2.16$ signal. Treatment of C531A CODH with CO for long periods of time (Figure 5) results in an EPR spectrum that is the combination of the $g_{ave} = 2.16$ signal and a slow-relaxing $S = 1/2$ signal with $g_{z,y,x} = 2.04, 1.93,$ and $1.89$ ($g_{ave} = 1.95$). Ambiguity about the origin of EPR-observable species was removed through analysis of Ni-deficient C531A CODH (Figure 9), where a slow-relaxing cluster (in addition to another faster-relaxing cluster) is observed at the same $g$ values as seen in C531A CODH treated with CO for 1 h (deconvoluted spectrum not shown). Therefore, the slow-relaxing cluster observed in C531A treated with CO for 1 h most probably arises from $[Fe_4S_4]_C^{1+}$. Its presence in addition to the $g_{ave} = 2.16$ resonance is argument against the $g_{ave} = 2.16$ signal arising from $[Fe_4S_4]_C$ spin-coupled in an unusual manner to $Ni^{2+}$ ($S = 1$). Treatment of C531A CODH with dithionite (Figure 6) produces a spectrum that is comprised of a fast-relaxing $[Fe_4S_4]^{1+}$ cluster in combination with the resonances observed when C531A CODH is treated with CO for long periods of time (Figure 5). The $\epsilon_{420}$ of dithionite-treated C531A CODH is identical to that of dithionite-treated wild-type CODH, suggesting that all $[Fe_4S_4]$ clusters are reduced. Under these conditions, the total spin for C531A CODH quantifies to nearly 3 spins/molecule ($2.80 \pm 0.10$ spins/molecule). Therefore, resonances arising from three separate paramagnetic species are present in the EPR spectrum. Two of these three paramagnetic species produce changes in $\epsilon_{420}$ and have relaxation properties similar to those of the $[Fe_4S_4]$ clusters observed in Ni-deficient C531A CODH shown in Figure 9. Thus, the third paramagnetic species, the $g_{ave} = 2.16$ signal, cannot arise from either $[Fe_4S_4]_C^{1+}$ or $[Fe_4S_4]_B^{1+}$.

**A Signal Similar to the $g_{ave} = 2.16$ Signal in C531A CODH Is Present in Hydrogenase With Its Origin in a [NiFe] Cluster.** While the $g_{ave} = 2.16$ signal cannot be arising from $[Fe_4S_4]_C$ or $[Fe_4S_4]_B$, a possible explanation of the source of the $g_{ave} = 2.16$ signal can be found in [NiFe] hydrogenases. The power- and temperature-optimized spectrum of the $g_{ave} = 2.16$ species (Figure 2B) of C531A CODH under nonsaturating conditions bears a resemblance to the spectrum of Ni-L signals of *C. vinosum* hydrogenase,[33,34] but with a slightly different $g_z$. Numerous paramagnetic nickel species have been observed in
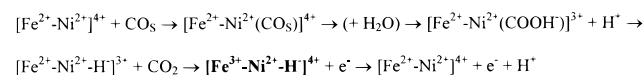
**Scheme 1**

$[Fe^{3+}-Ni^{3+}]^{6+}$ ($S = 1$ or $S = 0$) $\rightarrow$ $\mathbf{[Fe^{3+}-Ni^{2+}]^{5+}}$ ($S = 1/2$) $\rightarrow$ $[Fe^{2+}-Ni^{2+}]^{4+}$ ($S = 0$)

**Scheme 2**

$[Fe^{2+}-Ni^{2+}]^{4+}$ ($S = 1$ or $S = 0$) $\rightarrow$ $\mathbf{[Fe^{3+}-Ni^{0}]^{3+}}$ ($S = 1/2$) $\rightarrow$ $[Fe^{2+}-Ni^{0}]^{2+}$ ($S = 0$)

**Scheme 3**

$[Fe^{2+}-Ni^{2+}]^{4+} + CO_S \rightarrow [Fe^{2+}-Ni^{2+}(CO_S)]^{4+} \rightarrow (+ H_2O) \rightarrow [Fe^{2+}-Ni^{2+}(COOH^-)]^{3+} + H^+ \rightarrow$

$[Fe^{2+}-Ni^{2+}-H^-]^{3+} + CO_2 \rightarrow \mathbf{[Fe^{3+}-Ni^{2+}-H^-]^{4+}} + e^- \rightarrow [Fe^{2+}-Ni^{2+}]^{4+} + e^- + H^+$

[NiFe] hydrogenases. Generally, the enzymes are obtained in an inactive form (presumably $[Fe^{2+}-Ni^{3+}]^{5+}$), which exhibits an EPR observable $S = 1/2$ spectrum. Upon reduction, the enzyme passes through an EPR-silent state that is believed to be $[Fe^{2+}-Ni^{2+}]^{4+}$ ($S = 1$) on its way to another EPR observable ($S = 1/2$) state, which is believed to be $[Fe^{2+}Ni^{1+}]^{3+}$ or $[Fe^{2+}-Ni^{3+}-H^-]^{4+}$ and which is termed Ni-C (typical $g_{z,y,x} = 2.20, 2.16, 2.02$; $g_{ave} = 2.13$). Another possible $Ni^{1+}$ species, Ni-L, is obtained from the irradiation of the Ni-C species. The irradiation process is believed to dissociate a hydrogen atom from Ni-C. Ni-L has values typically in the region $g_z = 2.28-2.31$, $g_y = 2.13$, and $g_x = 2.03$, similar to the $g_{ave} = 2.16$ signal seen in C531A CODH. However, while the $g$ values of Ni-L are similar to the $g_{ave} = 2.16$ signal in C531A CODH, Ni-L is broadened by 6 G upon substitution with $^{61}Ni$, unlike the $g_{ave} = 2.16$ signal. Therefore, the EPR spectra of hydrogenases and C531A CODH have both similarities and differences that must be reconciled for a comparison to be meaningful.

The above differences between the $g_{ave} = 2.16$ signal in C531A CODH and similar resonances in hydrogenases can be reconciled if CODH contains a binuclear [FeNi] cluster (we will refer to the CODH cluster as [FeNi] and the hydrogenase clusters as [NiFe]) but with a different electron distribution. The metal analysis data presented in Table 1 supports the possibility of a binuclear [FeNi] cluster. However, instead of spin density residing on the Ni atom as it does in hydrogenases, in C531A CODH it resides on the Fe atom. The accompanying manuscript presents data indicating that the $g_{ave} = 2.16$ signal arises from a species that is catalytically relevant in CO oxidation and is the semireduced state of the putative [FeNi] cluster (i.e., the [FeNi] cluster has two redox couples). These two considerations suggest two possible schemes (where bold font indicates the possible origin of the $g_{ave} = 2.16$ signal). Scheme 1 cannot be ruled out but seems unreasonable because the redox potentials of such species would likely be higher than those observed in CODH and a $[Fe^{3+}-Ni^{3+}]^{6+}$ cluster likely would be unable to bind CO. Scheme 2 produces an $Fe^{3+}$ atom coupled to a highly reducing species ($Ni^0$). However, Scheme 2 can be modified, keeping in mind a reasonable catalytic mechanism for CO oxidation, by the incorporation of a hydrogen atom according to Scheme 3 (where the state producing the $g_{ave} = 2.16$ signal is shown in bold face). The inclusion of a hydrogen atom is reasonable, as the Ni-C and Ni-R states of [NiFe] hydrogenases are proposed to also have a bound hydrogen species.[35] Additionally, a pH dependence of the EPR properties of an analogous $g_{ave} = 2.16$ signal was reported for *C. thermoaceticum* CODH treated with thiocyanate. The pH dependence ($pK_a =$

(33) van der Zwaan, J. W.; Albracht, S. P. J.; Fontijn, R. D.; Roelofs, Y. B. M. *Biochim. Biophys. Acta* **1986**, *872*, 208−215.

(34) van der Zwaan, J. W.; Coremans, J. M. C. C.; Bouwens, E. C. M.; Albracht, S. P. J. *Biochim. Biophys. Acta Protein Struct. Mol. Enzymol.* **1990**, *1041*, 101−110.

(35) Schneider, K.; Erkens, A.; Müller, A. *Naturwissenschaften* **1996**, *83*, 78−81.

7.2 $\pm$ 0.1) roughly paralleled that of CO oxidation (p$K_a$ = 7.60 $\pm$ 0.2).[11] Further, several known inhibitors of CODH activity (CS$_2$, RCN, N$_3^-$)[32,36,37] are known to undergo intramolecular hydrogen insertion or transfer reactions at M$-$H$^-$ sites.[38]

The putative [Fe$^{3+}$-Ni$^{2+}$-H$^-$]$^{4+}$ state can be produced in the absence of the substrate CO (CO$_S$) in C531A CODH from an EPR unobservable [Fe$^{2+}$-Ni$^{2+}$]$^{4+}$ state ($S$ = 1, data presented in the accompanying manuscript). The Fe atom apparently remains low spin at all times. Low-spin ferric atoms display an $S$ = $^1/_2$ signal, while the Ni$^{2+}$-H$^-$ portion may be diamagnetic and EPR-silent. Therefore, a [Fe$^{3+}$-Ni$^{2+}$-H$^-$]$^{4+}$ cluster should have an $S$ = $^1/_2$ signal arising from the low-spin ferric atom. A $g_{ave}$ > 2 is generally observed for isolated low-spin ferric ions, and this is consistent with the $g_{ave}$ = 2.16 species in C531A CODH. Additionally, spin density on an Fe atom rather than a Ni atom may account for the relaxation properties of the $g_{ave}$ = 2.16 signal as a function of temperature (Figure 3), which are different from the relaxation properties of typical Ni$^{1+}$ paramagnets. The putative assignment of the $g_{ave}$ = 2.16 species as arising from a [FeNi] cluster is supported by reports of hydrogenase activity in *C. thermoaceticum* CODH.[39] We have also observed weak hydrogenase activity in *R. rubrum* CODH (data not shown). Additionally, small features observable in the spectrum of indigo carmine-poised C531A CODH ($g$ = 2.20, 2.17, and 2.00) may represent a fraction of the putative [FeNi] site with a different electronic distribution than the $g_{ave}$ = 2.16 species. These spectral features occur in positions similar to the spectral features of Ni-C ([Fe$^{2+}$-Ni$^{1+}$]$^{3+}$ or [Fe$^{2+}$-Ni$^{3+}$-H$^-$]$^{4+}$) observed in most [NiFe] hydrogenases (typical $g_{z,y,x}$ = 2.20, 2.16, 2.02; $g_{ave}$ = 2.13), providing additional evidence that the $g_{ave}$ = 2.16 feature arises from a [FeNi] cluster.

**The Role of Cys-531.** Using the hypothesis that the species producing the $g_{ave}$ = 2.16 signal is a [FeNi] cluster, we now ask why its presence is caused by replacing cys-531 with ala. The EPR spectrum of dithionite-treated, Ni-deficient C531A (Figure 9) displays only two reduced [Fe$_4$S$_4$] clusters, clearly seen from their differing relaxation properties as a function of temperature. Interestingly, even in the absence of Ni, [Fe$_4$S$_4$]$_C$ has unusual relaxation properties unlike those of typical all-cysteinyl liganded [Fe$_4$S$_4$] clusters, which are usually observable only below 35 K. [Fe$_4$S$_4$]$_C^{1+}$ is observable to 50 K, suggesting unusual iron ligation. However, the spectral properties of Ni-deficient C531A CODH are very similar to Ni-deficient wild-type CODH, suggesting that cys-531 is not involved in ligation to the [Fe$_4$S$_4$]$_C$ cluster.

If cys-531 is a ligand (terminal or bridging) to the putative [FeNi] cluster, removal would cause a change in reduction potential of the atoms within the cluster and would result in a significant redistribution of electron density relative to that of wild-type CODH. Changing the reduction potential of the putative [FeNi] cluster or redistributing electron density in an adverse manner within the cluster could then result in a kinetic barrier for the transfer of electrons to [Fe$_4$S$_4$]$_C$. However, in the accompanying manuscript (Part 2) we show that spin coupling of the $g_{ave}$ = 2.16 species ($S$ = $^1/_2$) with [Fe$_4$S$_4$]$_C^{1+}$ ($S$ = $^1/_2$) produces C$_{red1}$ in wild-type CODH. A dramatic redistribution of electron density in the C531A CODH variant is not observed. The probability that the $g_{ave}$ = 2.16 species is

present in active wild-type CODH in a spin-coupled form (see accompanying manuscript) argues against it being an improper form of the [FeNi] site.

On the basis of EXAFS studies,[40] *A. eutrophus* H16 [NiFe] hydrogenase is proposed to undergo changes in nickel ligation upon reduction from Ni-SI (proposed to be [Fe$^{2+}$-Ni$^{2+}$]$^{4+}$) to Ni-C (proposed to be [Fe$^{2+}$-Ni$^{3+}$-H$^-$]$^{4+}$ or [Fe$^{2+}$-Ni$^{1+}$]$^{3+}$). If cys-531 is a ligand in a more reduced state of the putative [FeNi] cluster in CODH, but not the state which produces the $g_{ave}$ = 2.16 signal, then a barrier will be introduced for the reduction from a possible [Fe$^{3+}$-Ni$^{2+}$-H$^-$]$^{4+}$ state to a [Fe$^{2+}$-Ni$^{2+}$-H$^-$)]$^{3+}$ ($S$ = 0) state. This could explain the inability of the putative [FeNi] cluster to be reduced in C531A CODH by dithionite (see Figure 6), contrary to what is observed in wild-type CODH and as presented in the accompanying manuscript. However, the $g_{ave}$ = 2.16 signal can be generated by treatment of fully oxidized (thionin-pretreated) C531A CODH with CO and subsequent titration with oxidized indigo carmine until a faint color of oxidized indigo carmine persists. This indicates that the putative [Fe$^{2+}$-Ni$^{2+}$-H$^-$]$^{3+}$ (i.e., fully reduced) state is accessible using substrate. Therefore it appears that C531A CODH can oxidize CO but cannot effectively transfer electrons to [Fe$_4$S$_4$]$_C$.

As Figures 5 and 6 show, both the $g_{ave}$ = 2.16 species and [Fe$_4$S$_4$]$_C^{1+}$ are manifest when C531A is treated with dithionite or with CO for long periods of time, but no trace of C$_{red1}$ is present. As spin coupling of the $g_{ave}$ = 2.16 species ($S$ = $^1/_2$) with [Fe$_4$S$_4$]$_C^{1+}$ ($S$ = $^1/_2$) is proposed to produce C$_{red1}$ in wild-type CODH, the absence of C$_{red1}$ indicates that the [Fe$_4$S$_4$]$_C^{1+}$ cluster and the proposed [Fe$^{3+}$-Ni$^{2+}$-H$^-$]$^{4+}$ site do not couple in C531A CODH. Further, the absence of [Fe$_4$S$_4$]$_C^{1+}$ in indigo carmine-treated C531A CODH reveals that the [Fe$_4$S$_4$]$_C^{2+/1+}$ couple is lower in potential than the [Fe$_4$S$_4$]$_C^{2+/1+}$ couple in wild-type CODH. Taking into account the lower potentials (relative to wild-type CODH) of the putative [FeNi] cluster and the [Fe$_4$S$_4$]$_C$ cluster in C531A CODH in combination with a lack of any observed C$_{red1}$ signals, we arrive at the conclusion that cys-531 is directly involved in the coupling of [FeNi] to [Fe$_4$S$_4$]$_C$. When the two clusters are not coupled, the potentials of both are lowered. Slow transfer of electrons from [FeNi] to [Fe$_4$S$_4$]$_C$ is possible, but it appears that a fast conduit of electron flow from the [FeNi] site to [Fe$_4$S$_4$]$_C$ is broken, and the two clusters are probably oriented at a slightly greater distance from each other than they are in wild-type CODH (as demonstrated by the lack of spin$-$spin interaction when both are reduced). However, the exact site to which cys-531 is bound in wild-type CODH remains unknown.

**A Nonsubstrate CO Molecule (CO$_L$) Is Bound to the [FeNi] Cluster in CODH.** Treatment of indigo carmine-poised C531A CODH with concentrations of CN$^-$ that produce *reversible* inactivation results in the total but reversible loss of the $g_{ave}$ = 2.16 species (Figure 7). The fact that the $g_{ave}$ = 2.16 species can be regained only upon CO treatment after CN$^-$ removal and that recovery of the $g_{ave}$ = 2.16 species correlates with the recovery of 90% of enzyme activity suggests that CN$^-$ displaces a bound CO (CO$_L$) molecule. It is probable that displacement of CO$_L$ with CN$^-$ changes the reduction potential of the [FeNi] cluster such that it is either in a more oxidized or in a more reduced state than that producing the $g_{ave}$ = 2.16 signal, when poised with indigo carmine. No additional resonances were observed in the EPR spectrum after CN$^-$ treatment

(36) Kumar, M.; Lu, W.-P.; Ragsdale, S. W. *Biochemistry* **1994**, *33*, 9769$-$9777.

(37) Kumar, M.; Ragsdale, S. W. *J. Am. Chem. Soc.* **1995**, *117*, 11604$-$11605.
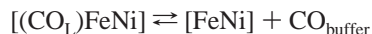
(38) Cotton, F. A.; Wilkinson, G. *Advanced Inorganic Chemistry*, 5th ed.; John Wiley & Sons: New York, 1988.

(39) Menon, S.; Ragsdale, S. W. *Biochemistry* **1996**, *35*, 15814$-$15821.

(40) Gu, Z.; Dong, J.; Allan, C. B.; Choudhury, S. B.; Franco, R.; Moura, J. J. G.; Moura, I.; LeGall, J.; Przybyla, A. E.; Roseboom, W.; Albracht, S. P. J.; Axley, M. J.; Scott, R. A.; Maroney, M. J. *J. Am. Chem. Soc.* **1996**, *118*, 11155$-$11165.

when the enzyme was poised with indigo carmine, with the exception of a very small quantity of a $[Fe_3S_4]^{1+}$ ($S = 1/2$) cluster, which is probably caused by the breakdown of $[Fe_4S_4]_C$ (data not shown).

The $CN^-$-binding studies suggest the possibility that a CO-bound form of the [FeNi] cluster is the "ready" form of both C531A and wild-type CODH. This possibility is supported by the following observations: (1) CO treatment of CODH after removal of activity-inhibiting micromolar $CN^-$ concentrations resulted in the restoration of CO oxidation activity (as determined by initial activity measurement), while CODH that was not CO-pretreated had very low initial activity. (2) CO preincubation of the as-isolated wild-type enzyme, and subsequent removal of unbound CO by gel-filtration chromatography, resulted in an enzyme with increased initial CO-oxidation activity relative to as-isolated CODH, which was not CO-pretreated. (3) Extensive handling of C531A CODH and subsequent poising with 95% reduced indigo carmine only produced the $g_{ave} = 2.16$ species in very low spin-quantity. Restoration of the $g_{ave} = 2.16$ species was possible upon treatment of C531A CODH with CO and subsequent fast poising with indigo carmine. (4) Extensive handling of wild-type CODH resulted in a much lower initial CO oxidation activity (10−90% diminished, depending upon handling time and method), which could be completely regained upon CO treatment as above. The above observations suggest that $[(CO_L)FeNi]$ equilibrates (with extensive handling) very slowly with buffer according to the following equation:

$$[(CO_L)FeNi] \rightleftarrows [FeNi] + CO_{buffer}$$

The inhibitory effect on activity of micromolar $[CN^-]$, concurrent with decreases in intensity of the $g_{ave} = 2.16$ signal, may be due to the displacement of a bound but nonsubstrate CO molecule ($CO_L$), creating the same effect as extensive handling, but at a faster rate. The presence of $CO_L$ at the [FeNi] site may explain the CO-dependent activation of $CN^-$-inhibited *R. rubrum* CODH observed by Ensign and Hyman in our lab.[28] A previous report by Kumar and Ragsdale[41] did not find a bound, exchangeable C site CO molecule observable in *C. thermoaceticum* CODH by FTIR spectroscopy. However, our preliminary data indicates that $CO_L$ does not readily exchange with $^{13}CO$ once bound in the *absence* of extensive handling (i.e., extensive column work, prep-gel concentration, etc.). Kumar and Ragsdale reported only the difference FTIR spectrum of CO-treated ($^{12}CO$ or $^{13}CO$) CODH minus CO-untreated CODH. Intrinsic $CO_L$ would be subtracted out. To prove $CO_L$ by this method, one must have CODH that has never been exposed to CO. This form of CODH is now available, and will be described in a future publication. Combining the proposed hydride and $CO_L$ ligation for the [FeNi] cluster, the $g_{ave} = 2.16$ signal is now described as arising from a $[(CO_L)Fe^{3+}-Ni^{2+}-H^-]^{4+}$ species.

**A CO-Bound [FeNi] Cluster Has Precedence in [NiFe] Hydrogenases.** If a $CO_L$-bound form of the [FeNi] cluster is the "ready"-form of C531A (and wild type) CODH, a comparison should be made to the behavior of the [NiFe] clusters of hydrogenases in the presence of CO. When the behavior of the [FeNi] and [NiFe] clusters in C531A CODH and hydrogenases in the presence of CO are compared, notable differences are evident. In most hydrogenases, exogenous CO is a reversible inhibitor. Obviously, in C531A and wild-type CODH, CO is the substrate (termed $CO_S$ to differentiate it from $CO_L$).

Concurrent with inhibition in hydrogenases are changes in their EPR spectra. Of particular relevance to C531A CODH are the spectral changes that occur in hydrogenases upon CO treatment of the Ni-C state (proposed to be $[Fe^{2+}-Ni^{1+}]^{3+}$ or $[Fe^{2+}-Ni^{3+}-H^-]^{4+}$, $S = 1/2$). For example, treatment of $H_2$-reduced *C. vinosum* hydrogenase with CO results in the appearance of another signal ($g_{z,y,x} = 2.12, 2.07, 2.02, g_{ave} = 2.07$) and in the concurrent decrease in Ni-C, indicating that CO binds to Ni-C to produce Ni-C(CO). The $g$ values of the CO-bound form of most hydrogenases ($g_{ave} = 2.07$) are, however, unlike the $g_{ave} = 2.16$ signal of C531A CODH. In most hydrogenases, CO dissociates from Ni-C(CO) upon illumination to yield another proposed $[Fe^{2+}-Ni^{1+}]^{3+}$ species referred to as Ni-L.[33] In C531A CODH, illumination has no effect upon the $g_{ave} = 2.16$ species (data not shown). However, treatment of the Ni-C state of *A. eutrophus* H16 hydrogenase with CO results in a Ni-C(CO) state with a spectrum similar to the $g_{ave} = 2.16$ signal of C531A CODH (and also to Ni-L signals in most hydrogenases), with $g_{z,y,x} = 2.35, 2.08, 2.01$ and $g_{ave} = 2.15$.[42] Like the $g_{ave} = 2.16$ signal of C531A CODH, the $g_{ave} = 2.15$ signal is insensitive to illumination. This hydrogenase maintains catalytic activity even in the presence of CO, suggesting a binding site for CO separate from the substrate ($H_2$) binding site. Additionally, the apparent slow rate of dissociation of CO from Ni-C(CO) in this hydrogenase is similar to that proposed for the $g_{ave} = 2.16$ species in *R. rubrum* C531A CODH. Similarly to the C531A CODH $g_{ave} = 2.16$ signal, the $g_{ave} = 2.15$ signal of Ni-C(CO) in *A. eutrophus* H16 hydrogenase is *not* significantly broadened in samples grown on $^{61}Ni$ (Dr. Klaus Schneider, personal correspondence). This comparison does not suggest that the overall ligation of the putative [NiFe]/[FeNi] clusters of *A. eutrophus* H16 hydrogenase and *R. rubrum* CODH is similar but that CO ($CO_L$ in CODH) and H may interact with the putative [FeNi]/[NiFe] clusters in a similar manner (i.e., similar sites).

**The Iron Atom of the [FeNi] Cluster Is at Least Partially Liganded by His Residues.** The $g_z$ (~2.33) of the $g_{ave} = 2.16$ species obtained at high resolution is comprised of what appears to be greater than four resonances (Figure 4). Previous reports of the $g_{ave} = 2.16$ signal in *C. thermoaceticum* did not reveal this hyperfine splitting; however, a temperature of 10 K and powers ranging from 40 to 100 mW were used with suboptimal modulation amplitudes. Under these conditions, the $g_{ave} = 2.16$ feature would be broadened by power saturation effects, and observation of hyperfine splitting of the $g_z = 2.33$ feature would not be possible. It is possible that there are more than three distinct species (similar to the Ni-L1/L2/L* seen in [NiFe] hydrogenases); however, it is more probable that there is nuclear hyperfine coupling due to interaction of the unpaired spin with nonzero nuclear spin(s). The most obvious candidates are one or more nitrogenous ($^{14}N$, $I = 1$) ligand(s), presumably histidinyl, and hydrogen ($^1H$, $I = 1/2$) directly interacting with the orbital containing the unpaired electron. It is possible that the hyperfine lines arise from a mixture of interactions with both of these ligand types, or only $^{14}N$ (necessarily more than one, as a single $^{14}N$ interaction would produce a three line pattern). The distances between the hyperfine lines within the 2.33 resonance are not equal and vary from approximately 17 to 24 G (shown in Figure 4 as "~A"; the actual hyperfine constants are difficult to accurately determine due to the overlapping nature of the lines). ENDOR experiments are planned to determine the exact origin of the hyperfine interac-

(41) Kumar, M.; Ragsdale, S. W. *J. Am. Chem. Soc.* **1992**, *114*, 8713−8715.

(42) Erkens, A.; Schneider, K.; Müller, A. *J. Biol. Inorg. Chem.* **1996**, *1*, 99−110.

11044   *J. Am. Chem. Soc., Vol. 121, No. 48, 1999*

*Staples et al.*

tion. The observed hyperfine splitting of the $g_{ave} = 2.16$ signal, in conjunction with the lack of $^{61}$Ni broadening, suggests that Fe of the putative [FeNi] cluster is liganded by at least one histidinyl ligand. The possibility of histidinyl ligands for the iron atom of the putative [FeNi] site is consistent with the lack of significant ligand to ferric charge-transfer bands in the UV−vis absorption spectrum upon production of the $g_{ave} = 2.16$ species. H265 is a good candidate for a ligand to the [FeNi] cluster as the H265V form of *R. rubrum* CODH lacks $C_{red1}$ and has very low activity. The anomolous EPR resonances reported in $g = 3-8$ region of the H265V variant probably arise from high-spin $Fe^{3+}$ forms of the Fe atom of the [FeNi] site.[43]

**Mössbauer Spectroscopy Has Hinted at the Presence of an Unusual Iron Site.** If a [FeNi] cluster exists, Mössbauer spectroscopy should provide evidence for a monomeric iron site in Ni-deficient CODH, and an unusual iron site should be observed in holo-CODH. Ni-deficient wild-type *R. rubrum* CODH does contain broad components absorbing around −3 to +3.5 mm/s velocity and accounting for 10% of the total absorption.[12] This value is very close to the $^1/_9$ necessary for a system comprised of $[Fe_4S_4]_C$, $[Fe_4S_4]_B$, and [FeX] (where X is the vacant Ni site). Holo wild-type *R. rubrum* CODH poised at −300 mV has been characterized by Mössbauer spectroscopy with a corresponding EPR sample reported.[12] The accompanying manuscript reports that $C_{red1}$ represents a spin-coupled system of the $g_{ave} = 2.16$ resonance with $[Fe_4S_4]_C^{1+}$ ($S = ^1/_2$). The accompanying manuscript also reports that, in holo wild-type CODH, the putative [FeNi] cluster can be reduced to an ($S = 0$) oxidation state, resulting in the uncoupling of $[Fe_4S_4]_C^{1+}$. Comparison of results presented in an unpublished manuscript by us to the reported EPR spectrum of *R. rubrum* CODH poised at −300 mV suggests that the [FeNi] cluster is in a mixture of redox states (possibly $[(CO_L)Fe^{2+}-Ni^{2+}-H^-]^{3+}$ ($S = 0$) and

$[(CO_L)Fe^{3+}-Ni^{2+}-H^-]^{4+}$ ($S = ^1/_2$)). The EPR spectrum, and thus Mössbauer spectrum, of $C_{red1}$ reported by Münck and co-workers[12] therefore arises from a composite of both coupled and uncoupled $[Fe_4S_4]_C^{1+}$. Nevertheless, Mössbauer of this sample at 100 K in the absence of applied field reveals two unusual components referred to as FCII and FCIII, which each comprise 7% of the total absorption for a sum of 14%. The value of 14% is also very close to the $^1/_9$ necessary for a system comprised of $[Fe_4S_4]_C$, $[Fe_4S_4]_B$, and [FeNi] clusters. FCII is reported to be similar to an $FeS_3N_2$ site on an $[Fe_4S_4]$ model complex constructed by Holm and co-workers.[44] This peta-coordinate site with a mixture of S and N ligands is consistent with the speculative coordination of the Fe in the [FeNi] site of C531A CODH based upon the hyperfine coupling results. It is possible that the work presented here and in the accompanying manuscripts will help to clarify the origins of the unusual iron sites observed in the Mössbauer spectra of *R. rubrum* CODH.

(43) Spangler, N. J.; Meyers, M. R.; Gierke, K. L.; Kerby, R. L.; Roberts, G. P.; Ludden, P. W. *J. Biol. Chem.* **1998**, *273*, 4059−4064.

(44) Ciurli, S.; Carrie, M.; Weigel, J. A.; Carney, M. J.; Stack, T. D. P.; Papaefthymiou, G. C.; Holm, R. H. *J. Am. Chem. Soc.* **1990**, *112*, 2654−2664.

(45) Ensign, S. A.; Ludden, P. W. *J. Biol. Chem.* **1991**, *266*, 18395−18403.